

Article

Heat Integration for Phenols and Ammonia Recovery Process of Coal Gasification Wastewater Considering Optimization of Process Parameters

Qiliang Ye ^{1,*}, Jiang Zeng ¹, Yuan Li ¹, Peiqing Yuan ¹ and Fuchen Wang ²¹ School of Chemical Engineering, East China University of Science and Technology, Shanghai 200237, China² Shanghai Engineering Research Center of Coal Gasification, East China University of Science and Technology, Shanghai 200237, China

* Correspondence: yql@ecust.edu.cn

Abstract: A heat integration optimization method that considers the changes in process parameters is proposed to find the global optimal process scheme for a coal chemical company's phenols and ammonia recovery process. The phenols and ammonia recovery process is simulated by Aspen Plus, and a programming method for heat exchanger networks synthesis that can simultaneously optimize process parameters and heat integration is constructed by Matlab. Taking the total annual cost as the objective function, the following process parameters are optimized: the hot feed temperature and cold/hot feed ratio of sour water stripper, the temperature of three-step partial condensation system, the feed temperature and column pressure of both solvent distillation column and solvent stripper. The result shows that, compared with the heat integration process under original process parameters, the new heat integration process saves 14.3% energy consumption and reduces the total annual cost by about 15.1%. The new heat integration process provides guidance for the optimization of the phenols and ammonia recovery process. The proposed heat integration optimization method based on changing process parameters is an effective and practical tool that offers good application prospects.

Keywords: coal gasification wastewater; heat exchanger network; heat integration; genetic algorithm



Citation: Ye, Q.; Zeng, J.; Li, Y.; Yuan, P.; Wang, F. Heat Integration for Phenols and Ammonia Recovery Process of Coal Gasification Wastewater Considering Optimization of Process Parameters. *Energies* **2022**, *15*, 9258. <https://doi.org/10.3390/en15239258>

Academic Editors: Jan Danielewicz and Krzysztof Rajski

Received: 7 November 2022

Accepted: 5 December 2022

Published: 6 December 2022

Publisher's Note: MDPI stays neutral with regard to jurisdictional claims in published maps and institutional affiliations.



Copyright: © 2022 by the authors. Licensee MDPI, Basel, Switzerland. This article is an open access article distributed under the terms and conditions of the Creative Commons Attribution (CC BY) license (<https://creativecommons.org/licenses/by/4.0/>).

1. Introduction

Coal gasification wastewater is the wastewater produced in the process of producing coal gas or replacing natural gas in a gasifier, and it mainly comes from washing, condensation, and fractionation sections [1]. The characteristics of this wastewater are high levels of toxicity and high concentration of pollutants, mainly containing phenols, ammonia, carbon dioxide, etc. It is difficult to achieve complete degradation of organic pollutants in the biochemical treatment process [2].

The combined technical route of chemical separation, biochemical treatment, and depth treatment is commonly used to treat highly concentrated organic wastewater containing phenols from coal gasification in industry [3–5]. The coal gasification wastewater contains concentrations of phenolic substances which will poison and inactivate the working flora in the biochemical treatment section. So, the phenols and ammonia recovery section of coal gasification wastewater before the biochemical treatment section has a non-negligible status. Its primary purpose is to recover most of the acidic substances, phenols, and ammonia in the coal gasification wastewater [6].

Two categories of the phenols and ammonia recovery process are roughly divided according to the order of phenols and ammonia removal, the two-column process based on the Lurgi coal gasification wastewater treatment process, and the single-column process based on the South China University of Technology wastewater treatment process. The former is not deaminated before phenols removal, resulting in alkaline wastewater, which reduces the efficiency of polyphenol removal [7]. The latter can remove the crude phenols

from the wastewater better but requires a large amount of medium- and high-pressure steam [8].

In order to meet the requirements of green chemistry and zero pollution emission, there is a need to develop a heat integration process that can save energy and accomplish the wastewater purification index at the same time. Many optimal processes have been proposed by researchers from the perspective of energy conservation, which indicates that the existing processes have great potential to reduce energy consumption through further process optimization and heat integration. Gai et al. [9] proposed two options for heat integration between solvent distillation column and solvent stripper based on the wastewater treatment process of South China University of Technology, among which the depressurized heat integration process and the pressure-swing heat integration process can save 18.6% and 18.2% of energy consumption, respectively. Cui et al. [10] obtained a new heat integration process by thermally integrating the sour water stripper column and solvent recovery system, saving 30.9% of energy consumption. In addition, the application of heat pumps has been extensively studied in the heat integration of phenols and ammonia recovery process. Chen et al. [11] analyzed the feasibility of steam recompression process using Grand Composite Curve and designed a new integration process. The final process saves USD 1.095 million in total annual utility consumption. Zahid [12] used Aspen Hysys to design the vapor recompression scheme of a sour water stripping unit in a refinery. Compared with the traditional design, the proposed vapor recompression design can reduce the demand for cooling and heating facilities by 90% and 22%, respectively. Gai et al. [13] used the flashing mechanical vapor recompression heat pump to reduce the energy consumption of sulfur-containing wastewater.

The above research demonstrated the feasibility and effectiveness of heat integration. However, the process can still be further improved. Jin et al. [14] pointed out that the traditional heat integration design program needs to start with a good process design; that is, to optimize the design parameters of the process first, and then conduct the heat integration design. This may lead to the omission of some more competitive solutions. Therefore, the simultaneous optimization of process parameters and heat integration has attracted more and more attention from scholars [15–18]. There have been many studies applying this method to actual processes. Huang et al. [19] used an extended Duran–Grossmann model to optimize the heat exchanger network of the coal-to-SNG process. By optimizing the operating parameters, the exergy efficiency of the coal-to-SNG plant increased by 1.28% compared to the original industrial plant. Khor et al. [20] addressed the flowsheet optimization of the synthesis of a petroleum refinery to attain an optimal heat-integrated configuration or topology.

Despite the successful application of some processes of the simultaneous optimization of process parameters and heat integration, the use of simultaneous optimization methods in the process of phenols and ammonia recovery is practically not described in the literature. Therefore, in this study, considering the high energy consumption and high cost of the wastewater treatment process of a coal chemical company, the process technology is improved. The whole process simulation of the phenols and ammonia recovery process is completed by Aspen Plus according to the specific data of the coal chemical company. A heat exchanger network synthesis program that can simultaneously optimize process parameters and heat integration schemes is constructed. The total annual cost (TAC) is used as the objective function, then the influence of some operating parameters on the heat exchanger network is analyzed. This paper is presented in the following order: the second section describes and simulates the process of phenols and ammonia recovery; the third section provides the mathematical model of heat integration; the fourth section presents the results; the last section summarizes the conclusions.

2. Process Description and Simulation

The process flow of phenols and ammonia recovery in the coal chemical plant is shown in Figure 1. This process contains a single pressurized column to achieve simultaneous acid

stripping from the column top and deamination from the side line. The phenols-containing wastewater, after deacidification and deamination, enters the top of an extraction column, and the methyl isobutyl ketone (MIBK) extractant enters the extraction column from the bottom. MIBK and the wastewater are in continuous counter-current contact, and the phenols-containing MIBK comes out from the top of the extraction column, while the dephenolized wastewater is discharged from the bottom. The extraction solution from the top of the extraction column is pumped into a solvent distillation column equipped with reboiler, and the raffinate is pumped into a solvent stripper.

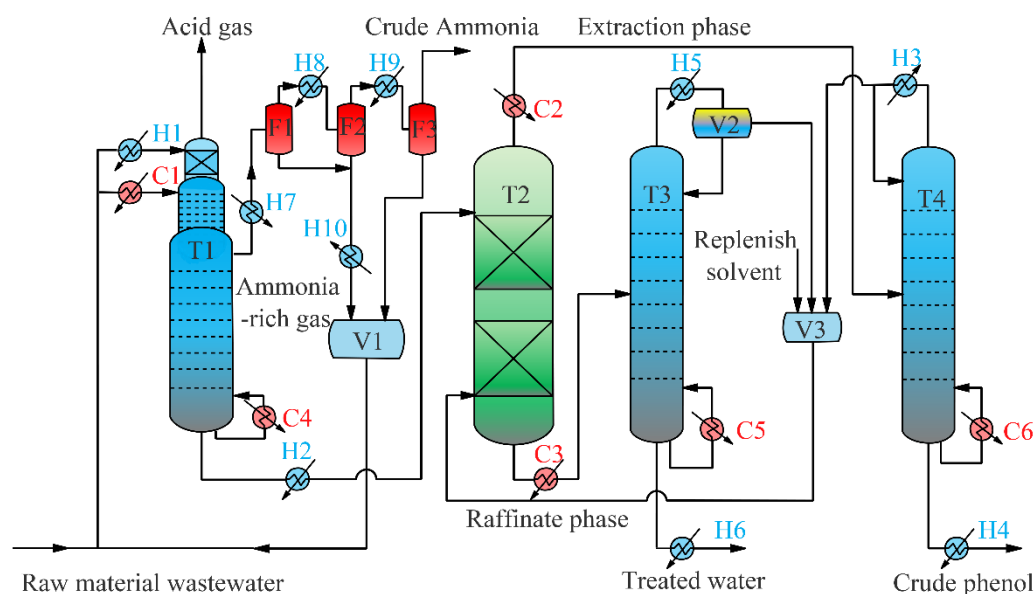


Figure 1. Flow chart of phenols and ammonia recovery process. T1: Sour water stripper; T2: Extraction column; T3: Solvent stripper; T4: Solvent distillation column; F1~3: Flash tanks; V1~3: Storage tanks; H1~10: Cooler; C1~6: Heater.

The ELECNRTL thermodynamics models in Aspen Plus are used to provide properties database [21]. Based on industrial data, the feed composition is shown in Table 1.

Table 1. Wastewater feed composition.

Components	H ₂ O	Phenol	Hydroquinone	NH ₃	CO ₂	H ₂ S
wt%	96.18	1.16	0.23	2.12	0.54	20 ppm

To meet the biochemical treatment requirements [10,22], the design specifications of each output product are stipulated as follows.

- (1) In order to avoid pipeline blockage, the compositions of water and ammonia in the acid gas at the top of the sour water stripper should be less than 3 wt% and 1.5 wt%, respectively.
- (2) The purity of crude ammonia product should reach 98 wt% after the three-step partial condensation system.
- (3) After the treatment of phenols and ammonia removal, the concentrations of total phenols, ammonia, and hydrogen sulfide in the wastewater are reduced to below 500, 150, and 50 mg/L, respectively.
- (4) MIBK should be reduced to 5 mg/L in the bottom discharge of solvent stripper.
- (5) The MIBK in the crude phenols product at the bottom of solvent distillation column should be less than 0.2 wt%.

- (6) In order to recover and utilize the solvent MIBK, the concentration of MIBK in the recovered stream at the top of solvent stripper and solvent distillation column should be greater than 97 wt%.

In order to match stream data with factory data and regulations as much as possible, the operating parameters of stripper and distillation columns are shown in Table 2.

Table 2. Operating parameters of the stripper and distillation columns.

Name	Soul Water Stripping Column	Solvent Stripping Column	Solvent Distillation Column
Number of stages	55	6	19
Distillate rate/kg·h ⁻¹	530	2540	13,000
Reflux ratio	/	/	0.2
Pressure/bar	6/6.05	1.03/1.04	1.03/1.05
Feed stages	1 #/5 #	1 #	12 #

stands for column plate serial number.

After the simulation of the whole process is completed, the simulation results are compared with the actual industrial data, as shown in Table 3. The results show that the simulated outlet temperature and pressure of each column are consistent with the actual operating conditions, which verifies the reliability of the simulation results.

Table 3. Comparison of simulation values and actual parameters.

Equipment Number	Indicator	Actual Value	Simulated Value
T1	Top temperature/°C	40~120	73
	Sideline temperature/°C	152	151
	Bottom temperature/°C	162	159
T2	Top temperature/°C	40 ± 5	38
	Bottom temperature/°C	40 ± 5	38
T3	Top temperature/°C	93	86
	Bottom temperature/°C	101	99
T4	Top temperature/°C	100 ± 10	93
	Bottom temperature/°C	200 ± 10	201

The heat exchanger information obtained from the simulation is organized as shown in Table 4. The parameters of each heat exchanger consist of three parts: initial temperature, target temperature, and required heat load. They will be imported into the heat exchanger network design model as input variables for the program programmed by Matlab.

Table 4. Information on the heat exchanger obtained from the simulation.

No.	Stream Name	Initial Temperature °C	Target Temperature °C	Heat Load kW
H1	Stripper cold feed	37	35	60.6
H2	Stripper bottom outlet	159	40	13,769.2
H3	Solvent distillation column condenser	113	93	1934.5
H4	Solvent distillation column bottom outlet	201	55	97.0
H5	Solvent stripper condenser	86	55	574.2
H6	Solvent stripper bottom outlet	99	50	5894.8
H7	1st ammonia-rich gas condenser	151	138	4585.5
H8	2nd ammonia-rich gas condenser	138	106	950.8
H9	3rd ammonia-rich gas condenser	106	40	322.1
H10	Ammonia condensate to tank	130	60	775.5
C1	Stripper hot feed	37	146	11,118.2
C2	Solvent distillation column feed	38	99	834.6
C3	Solvent stripper feed	38	87	5448.5
C4	Stripper reboiler	159	159	10,424.3
C5	Solvent distillation column reboiler	201	201	1712.8
C6	Solvent stripper reboiler	99	99	2136.7

3. Methodology of Heat Integration

3.1. Problem Description

Ten hot streams and six cold streams (containing three vapor flows) were matched to each other, supplemented by four sizes of utilities, including cooling water, 0.6 MPa low-pressure steam, 1.5 MPa medium-pressure steam, and 2.8 MPa medium-pressure steam, to obtain the heat exchanger network solution with the lowest total annual cost.

3.2. Objective Function

The objective function of the integrated heat exchanger network problem is total annual cost function (*TAC*) calculated under the selected heat exchanger network, which contains two parts: annual capital cost and operating cost [23,24]. The operating cost contains the cost of steam and cooling water consumed during the operation of the complete heat exchanger network equipment, and the capital cost is simplified to the cost of the column shell and heat exchanger equipment. The specific formula is shown below.

$$TAC = \frac{C_{hex} + C_{col}}{\text{payback period}} + ANC \cdot \text{year} \quad (1)$$

where C_{hex} denotes the equipment cost of the heat exchanger in the system. ANC denotes the consumption cost of the utilities in the system. The specific calculation method can be referred to the objective function equation of the heat exchanger network proposed by Lewin [25].

$$C_{hex} = \sum_{k=1}^{n_s} (A_0 + A_1 \cdot S_k^m) \quad (2)$$

$$ANC = A_2 \sum_{s1=1}^{n_{u1}} H_{s1} + A_3 \sum_{s2=1}^{n_{u2}} H_{s2} + A_4 \sum_{s3=1}^{n_{u3}} H_{s3} + A_5 \sum_{s4=1}^{n_{u4}} H_{s4} \quad (3)$$

n_s denotes the number of heat exchangers in the heat exchanger network. $n_{u1} \sim n_{u4}$ show the number of flows using cooling water, 0.6 MPa low pressure steam, 1.5 MPa medium pressure steam, and 2.8 MPa medium pressure steam, respectively. S represents the heat transfer area of a particular heat exchanger in m^2 . H indicates the amount of utility consumption used for a particular flow in kJ/h . $A_{0\sim5}$ express the economic factors of the heat exchanger equipment and each of the utility, and the specific values are shown in Table 5 [10,26].

Table 5. Economic factor values for heat exchanger equipment and utilities.

A_0	A_1	m	A_2 $\times 10^{-6}$ USD/kJ	A_3 $\times 10^{-6}$ USD/kJ	A_4 $\times 10^{-6}$ USD/kJ	A_5 $\times 10^{-6}$ USD/kJ
0	7296	0.65	4.43	7.78	8.22	8.22

C_{col} denotes the cost of the shell equipment for the distillation columns, which is calculated as follows.

$$C_{col} = 17640D^{1.066}(0.61N_T + 3)^{0.802} \quad (4)$$

D denotes the design inner diameter of the distillation column and N_T represents the theoretical number of stages of the distillation column. The payback period is calculated at three years, and the annual equipment work time is 8000 h.

3.3. Material Balance and Energy Balance

The structure of the heat exchanger network consists of several heat exchangers that can perform a thermal coupling between different streams. Each heat exchanger must follow the laws of material balance and energy balance. As shown in Figure 2, $t'_{h,ijk}$ and $t''_{h,ijk}$ indicate the inlet and outlet temperatures of the heat stream in the heat exchanger

codenamed ijk (i represents the cold stream code, j represents the hot stream code, and k represents the number of stages in which it is located), respectively, and similarly $t'_{c,ijk}$ and $t''_{c,ijk}$ respectively represent the inlet and outlet temperatures of the cold stream in the heat exchanger code-named ijk . $T_{h,j}^I$ and $T_{h,j}^T$ denote the initial and target temperatures of heat stream j , respectively. $T_{c,i}^I$ and $T_{c,i}^T$ represent the initial and target temperatures of cold stream i , respectively. After matching the hot and cold streams, the streams that still did not reach the heat transfer target were heat exchanged with suitable utilities in the auxiliary heat exchanger to achieve the final heat transfer requirements. $t'_{hu,j}$ and $t''_{hu,j}$ represent the inlet and outlet temperatures of heat stream j in the corresponding auxiliary heat exchanger, respectively. $t'_{cu,i}$ and $t''_{cu,i}$ denote the inlet and outlet temperatures of the cold stream i in the corresponding auxiliary heat exchanger, respectively.

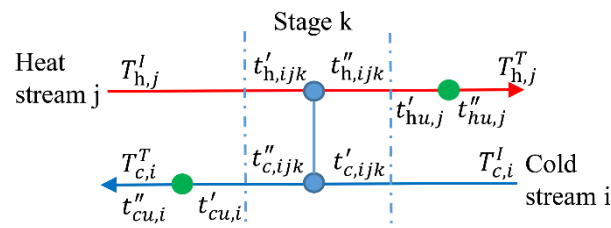


Figure 2. Heat transfer model for stream matching.

3.3.1. Energy Balance for Each Streams

In the heat exchanger network, the target heat exchange to be achieved by each stream is fixed, and the heat exchange is shared by each heat exchanger in the stream. Therefore, the energy balance equation for each stream is as follows.

$$\text{Heat stream : } Q_{h,j} = \sum_{k=1}^{n_R} \sum_{i=1}^{n_C} Q_{ijk} + Q_{hu,j} = W_{h,j} (T_h^I - T_h^T) \quad (5)$$

$$\text{Cold stream : } Q_{c,i} = \sum_{k=1}^{n_R} \sum_{j=1}^{n_H} Q_{ijk} + Q_{cu,i} = W_{c,i} (T_c^T - T_c^I) \quad (6)$$

Q_{ijk} denotes the heat exchange of heat stream j and cold stream i at the heat exchanger on stage k . If there is no heat exchanger at this position, it is specified that $Q_{ijk} = 0$. $W_{h,j}$ and $W_{c,i}$ represent the heat capacity flow rates of heat flow j and cold flow i , respectively.

3.3.2. Energy Balance for Heat Exchangers

A heat exchanger is an equipment that transfers part of the heat from one hot stream to another cold stream. In this study, only the split of heat streams was allowed to simplify the structure of the heat exchanger network. According to the law of energy conservation, the heat loss of the hot stream should be equal to the heat absorbed by the cold stream, so the energy balance formula of the heat exchanger is as follows.

$$Q_{ijk} = y_{ijk} \cdot W_{h,j} (t'_{h,ijk} - t''_{h,ijk}) = W_{c,i} (t''_{c,ijk} - t'_{c,ijk}) \quad (7)$$

where y_{ijk} denotes the i -th split of heat stream j at the k -th level to match cold stream i . If the j -th heat stream is not matched with the i -th cold stream at the k -th level, then $y_{ijk} = 0$.

3.3.3. Material Balance at the Diversion Node

Each heat stream can theoretically be divided into at most n_C shares of diversion in each stage. Then, the material balance at the diversion node is given by

$$\sum_{i=1}^{n_C} y_{ijk} = 1 \quad (8)$$

3.3.4. Energy Balance at the Merge Node

At each stage of one heat stream, the divided n_C streams of heat stream are reunited after exchanging energy with the corresponding n_C cold streams, respectively. Then, the energy balance equation at the merging node is as follows.

$$W_{h,j} \cdot t_{j,k} = \sum_{i=1}^{n_C} (y_{ijk} \cdot W_{h,j} \cdot t''_{h,ijk}) \quad (9)$$

where $t_{j,k}$ denotes the temperature of the heat stream entering the next stage after merging the heat stream j through the k -th stage. After calculating the exit temperature of the heat stream through the heat exchanger, the temperature of the heat stream in the next stage can be calculated by the above equation.

3.4. Thermodynamic Constraints

The heat exchangers mentioned in this paper are assumed to be counterflow heat exchangers. For counterflow heat exchangers, the temperature difference on both sides must meet the minimum driving force constraint.

$$t'_{h,ijk} - t''_{c,ijk} \geq \Delta T_{min} \quad (10)$$

$$t''_{h,ijk} - t'_{c,ijk} \geq \Delta T_{min} \quad (11)$$

where ΔT_{min} represents the minimum driving force of the counterflow heat exchanger.

3.5. Area Calculation of Heat Exchanger

According to the heat exchange of each heat exchanger and the inlet and outlet temperature of the corresponding hot and cold streams, the area of the heat exchanger can be calculated as follows

$$Q_{ijk} = u \cdot S_{ijk} \cdot \Delta T_m \quad (12)$$

$$\Delta T_m = \frac{(t''_{h,ijk} - t'_{c,ijk}) - (t'_{h,ijk} - t''_{c,ijk})}{\ln \left\{ \frac{(t''_{h,ijk} - t'_{c,ijk})}{(t'_{h,ijk} - t''_{c,ijk})} \right\}} \quad (13)$$

where u represents the heat transfer coefficient. For cooled heat exchanger, $u = 0.852 \text{ kW} / (\text{K} \cdot \text{m}^2)$. For re-boiling heat exchangers, $u = 0.568 \text{ kW} / (\text{K} \cdot \text{m}^2)$. If the cold and hot streams are vapor streams, and there is little temperature change before and after heat exchange, then ΔT_m is taken as the difference between the two.

3.6. Algorithm Implementation

The stage-wise superstructure model proposed by Yee [27] was used as the heat exchanger network model. A two-layer nested optimization structure was adopted in the algorithm [17]. The discrete variables represented by heat exchanger network structure were optimized in the upper layer using genetic algorithm (GA). The continuous variables (split flow rate and exchanger heat load) were optimized in the lower layer through particle swarm algorithm (PSO). The structural characteristics of each heat exchanger network were expressed in the algorithm by the incidence matrix [20]. The independent and dependent variables were obtained by structure identification of the heat exchanger network incidence

matrix [28]. The specific steps of this hybrid genetic algorithm for heat exchanger network design are given in Figure 3.

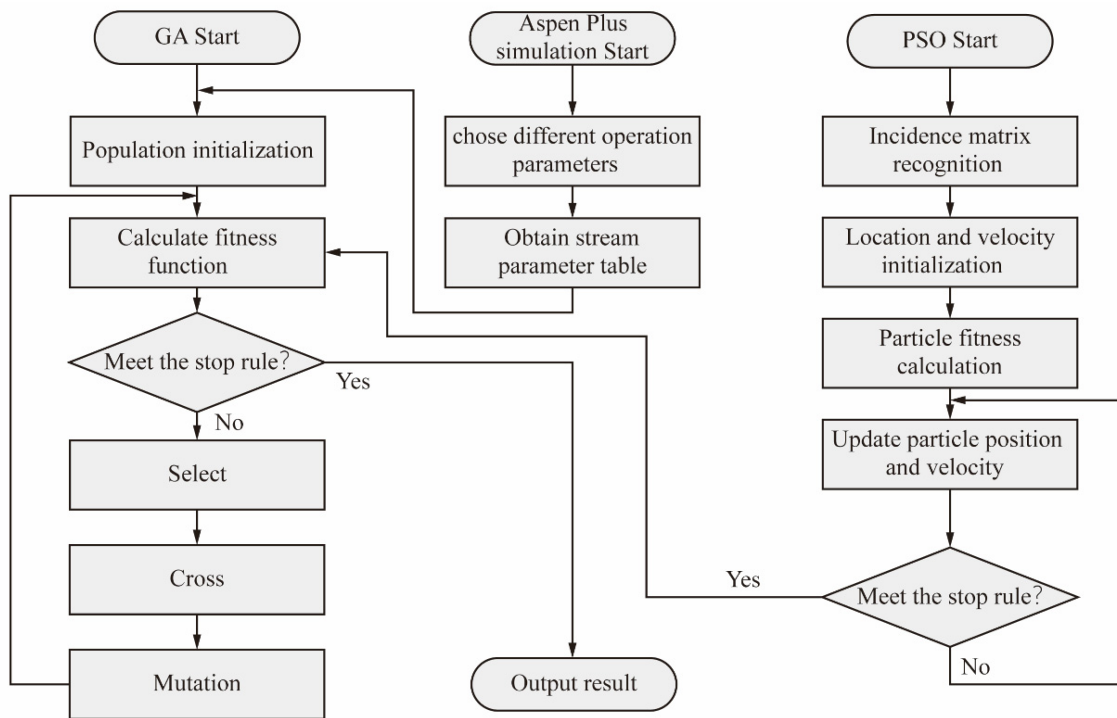


Figure 3. Heat exchange network design procedure steps.

The program runs in the following steps: after receiving the heat exchanger data from Aspen Plus, it first enters the PSO algorithm to complete the optimization of the heat exchanger parameters and then enters the GA algorithm to achieve the optimization of the heat exchanger network system by selection, crossover, and mutation.

4. Results and Discussions

The algorithm’s operation process is shown in Figure 4.

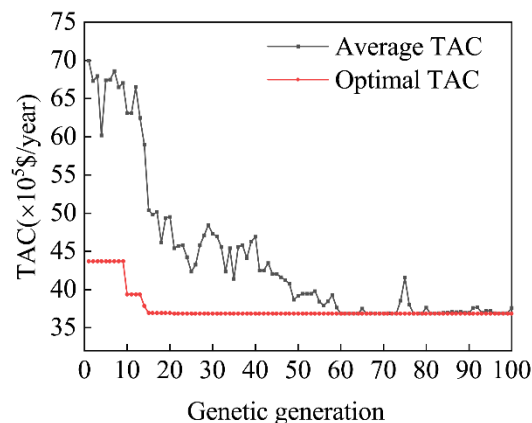


Figure 4. The running process of the algorithm.

As can be seen from Figure 4, after 15 generations of genetic inheritance, the individuals with optimal TAC are reproduced in the population. These individuals continue to develop and grow in the subsequent evolution, so that the average TAC of the population reaches the optimal TAC level after 60 generations of genetic inheritance and remains

unchanged afterward. It indicates that the established hybrid genetic algorithm has a strong convergence ability. Herein, the effects of some process parameters on the total annual cost of heat integrated process are analyzed.

4.1. Effects of Column Pressure in Solvent Distillation Column and Solvent Stripper

Cui et al. mentioned that the heat integration between these two columns could be accomplished by adjusting the pressure of the solvent distillation column and the solvent stripper [9]. In this paper, the effect of two column pressures on the optimization of the heat exchanger network is discussed. The process simulation under changing pressure conditions of the two columns was first completed using Aspen Plus, and the simulated data were imported by separate operations. The final optimization results are shown in Figure 5.

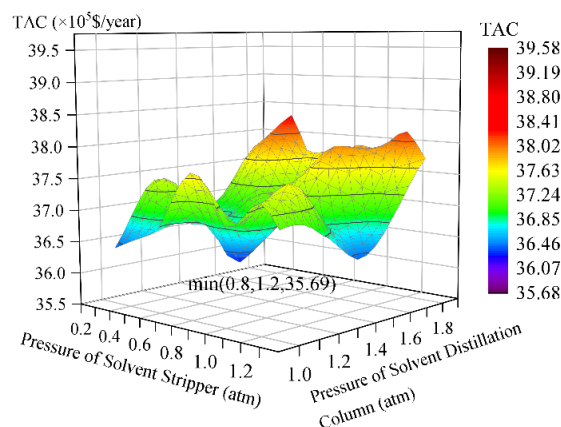


Figure 5. Effect of column pressure of solvent stripper and solvent distillation column on the total annual cost of the heat integration process.

Changing the pressure of solvent distillation column and solvent stripper will affect initial temperature, target temperature, and required heat load of some heat exchangers, thus forcing the hybrid genetic algorithm to seek a new optimal heat exchanger network structure. From Figure 5, it can be seen that when the pressures of solvent stripper and solvent distillation column are set to 0.8/1.2 atm, respectively, the total annual cost of the optimal heat exchanger network reaches the lowest.

The total annual cost of the heat integration process, on the other hand, is only slightly affected by adjusting the pressure of the twin columns, as shown in Figure 5, which is consistent with Cui et al.'s findings [9] in the literature. Therefore, this shows that there is a limit to the heat distribution and temperature distribution in the process section by adjusting the parameters in the column.

4.2. Effect of Cold-to-Hot Feed Ratio and Hot Feed Temperature

The raw material is divided into two streams before entering the sour water stripper. One stream enters the top of the column as a cold stream and the other stream is heated and enters the middle section of the column. The cold-to-hot feed ratio and the hot feed temperature affect the reboiler heat load of the sour water stripper. If the cold-to-hot feed ratio increases or the hot feed temperature decreases, the reboiler heat load required to complete the product indicators will increase. Usually, hot feed is preheated by matching with other streams, so the changes in cold-to-hot feed ratio and hot feed temperature on the total annual cost after heat exchanger network structure optimization were analyzed, as shown in Figure 6.

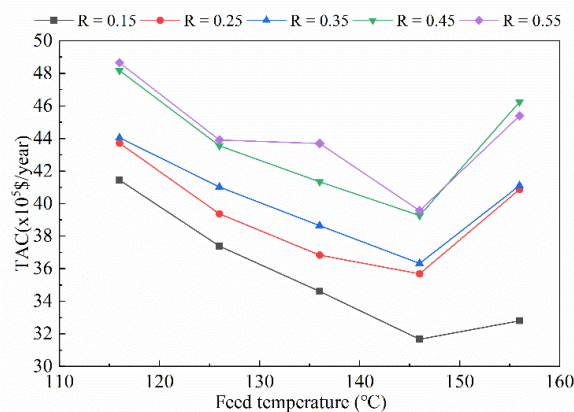


Figure 6. Effect of cold-to-hot feed ratio and hot feed temperature of sour water stripper on total annual cost of heat integration process.

It can be obviously seen from Figure 6 that the total annual cost after heat integration gradually increases as the cold-to-hot feed ratio continues to increase. As the hot feed temperature increases, the total annual cost after heat integration decreases and then increases. At a hot-to-cold feed ratio of 0.15 and a hot feed temperature of 146 °C, the total annual cost after heat integration is the lowest.

Sufficient heat exchange needs to be provided to drive the separation of the products, which includes the reboiler heat load and the feed heat load. The feed heat load is better integrated by the heat exchanger network than the reboiler heat load. In other words, the more heat required to separate the product that is provided by the heat exchange outside the column, the more easily the heat can be used in the heat exchanger network. It can also be seen from the analysis in Section 4.1 that stripping the required heat from the column is actually a means of avoiding reforming the heat distribution and temperature distribution by adjusting the parameters in the column.

4.3. Effect of the Temperature of the Three-Step Partial Condensation System

According to the literature, the temperature of three condensers affects not only the purity of crude ammonia gas, but also the energy consumption of the sour water stripper [8]. Among them, the first and second condensers together affect the heat load of the sour water stripper, and the third condenser mainly affects the purity of the extracted crude ammonia gas. The temperature of the third stage condenser must be set at about 40 °C to ensure that the purity of crude ammonia is greater than 98 wt%. The effect of the temperature of the first and second stage condensers on total annual cost is shown in Figure 7.

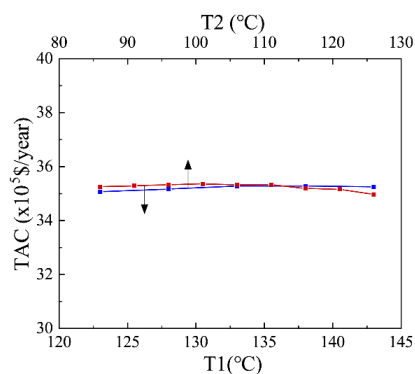


Figure 7. Effect of the temperature of the first and second condensers on the total annual cost of the heat integration process. As indicated by the arrow, the red line represents the variation of TAC with the temperature of the first condenser, while the blue line represents the variation of TAC with the temperature of the second condenser.

As shown in Figure 7, although the temperature of the first and second condensers affect the heat load of the sour water stripper, the effect on the overall phenols and ammonia recovery process is negligible. Such an observation may be due to the amount of ammonia extracted from the side lines being smaller compared to the amount of wastewater extracted from the bottom of the column (mass ratio of about 1:10). The heat load required by the three subsequent condensers is much smaller than the heat load of the heat exchangers on the other main roads, so the impact on the overall heat exchanger network is negligible.

4.4. Effect of the Feed Temperature in Solvent Stripper and Solvent Distillation Column

The effect of feed temperature of solvent stripper and solvent distillation column on the total annual cost of phenols and ammonia recovery process for coal gasification wastewater after heat integration was investigated, and the results are shown in Figure 8.

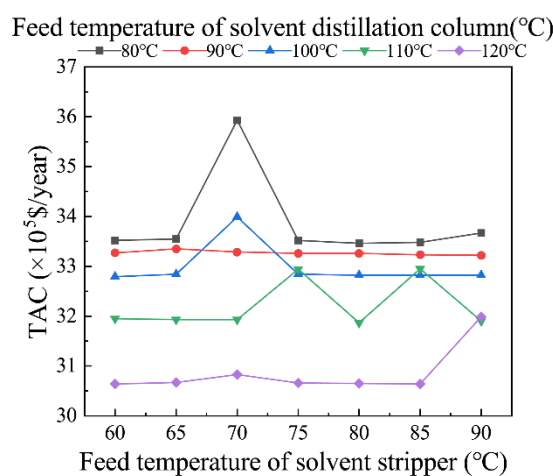


Figure 8. Effect of feed temperature of solvent stripper and solvent distillation columns on total annual cost of heat integration process.

Figure 8 presents that the feed temperature of the solvent stripper has little effect on the total annual cost, while the total annual cost gradually decreases as the feed temperature of the solvent distillation column increases. When the feed temperatures of the solvent stripper column and the solvent distillation column are set to 85/120 °C, respectively, the total annual cost of the phenols ammonia recovery process after heat integration is the lowest.

From the perspective of the whole process, the material flow rate that is required to be treated by the solvent distillation column is larger than the solvent stripper, and more heat needs to be provided, so the total annual cost after heat integration is more sensitive to the heat distribution of the solvent distillation column.

4.5. Summary

Through the previous analysis, it can be seen that the process parameters that can significantly affect the total annual cost of heat integration process are cold to hot feed ratio and hot feed temperature of the sour water stripper, column pressure, feed temperature of solvent distillation column, and column pressure of the solvent stripper.

Two ideas for implementing heat integration and simultaneous process parameter optimization for chemical processes using column equipment may be obtained from the analysis of the impact of the aforementioned factors on the annual total cost:

- (1) Optimize the heat distribution and temperature distribution in the process by optimizing the conditions outside the tower as far as possible;
- (2) Optimize the heat exchange equipment on the main material flow with large flow rate as far as possible.

In this phenols and ammonia recovery process, the optimal parameters at the lowest total annual cost were obtained as shown in Table 6.

Table 6. Optimal parameters at the lowest total annual cost.

Name	Design Parameters	Original Process	New Process	Unit
Sour water stripper	Ratio of cold feed to hot feed	0.25	0.15	/
	Hot feed temperature	135	146	°C
Three-step partial condensation system	The first stage condensation temperature	138	138	°C
	The second stage condensation temperature	106	106	°C
	The third stage condensation temperature	40	40	°C
Solvent stripper	Pressure	1.0	0.8	atm
	Feed temperature	90	85	°C
Solvent distillation column	Pressure	1.0	1.2	atm
	Feed temperature	100	120	°C

At this point the incidence matrix is:

$$\begin{bmatrix} 2 & 0 & 4 & 0 & 0 & 0 \\ 7 & 7 & 9 & 0 & 0 & 2 \\ 0 & 0 & 3 & 0 & 0 & 0 \end{bmatrix}$$

The corresponding heat exchanger network structure is shown in Figure 9, containing seven heat exchangers, six coolers, and three heaters, consuming 10,668 kW of cold utilities and 13,444 kW of heat utilities, with a total annual cost of 306,400 USD/year.

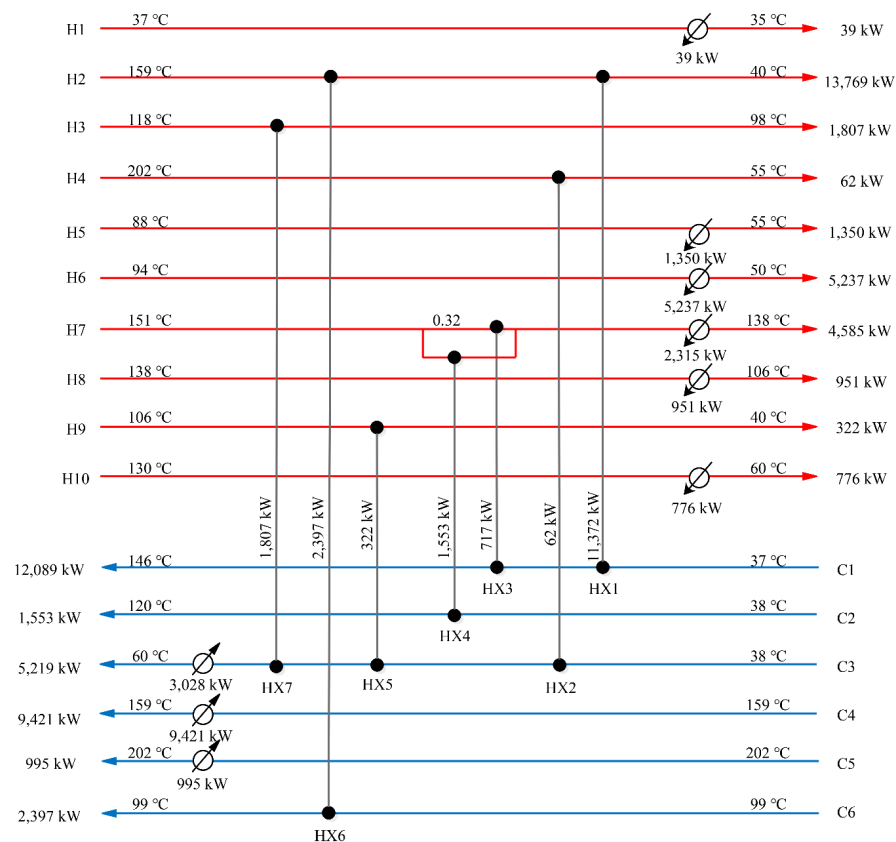


Figure 9. Final heat exchange network structure. The red line represents the hot streams for heating, the blue line represents the cold streams for cooling, and the solid circle represents the heat exchanger. The arrow indicates the direction of heat transfer.

According to the obtained heat exchanger network structure, the process simulation of phenols ammonia recovery process of coal gasification wastewater with heat exchanger network structure was completed on Aspen Plus. The schematic diagram of the heat exchanger network streams direction is shown in Figure 10.

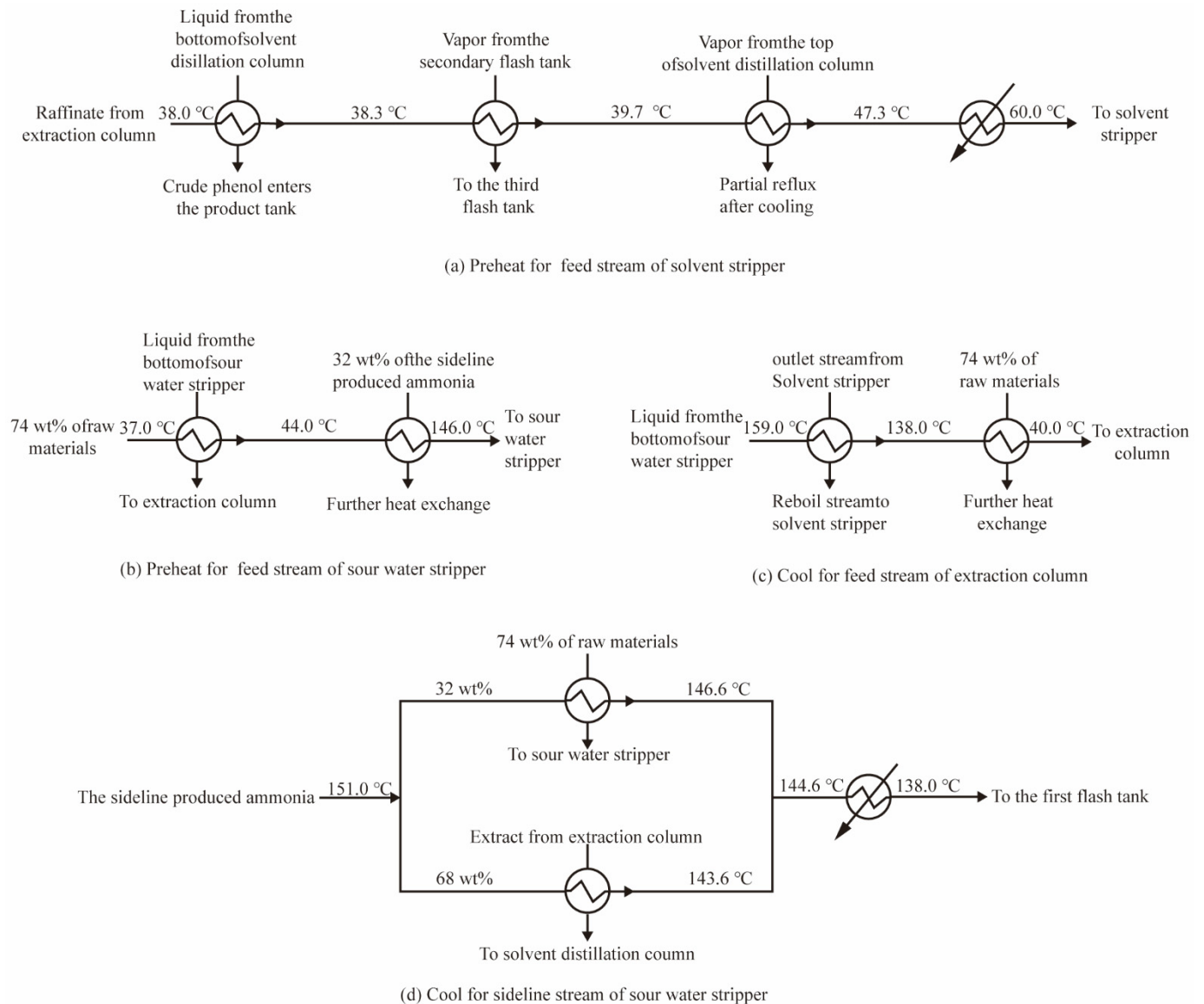


Figure 10. Schematic diagram of the stream direction in the heat exchange network. The arrow indicates the direction of heat transfer.

The main streams of the heat exchanger network are divided into four routes.

- The extracted residue from the extraction column was heat exchanged with the bottom discharge of the solvent distillation column, the gas phase from the second flash tank, and the gas phase discharge from the top of the solvent distillation column, and then heated to 60 °C by the auxiliary heater and fed into the solvent stripper.
- The raw material is divided into 74 wt% and heated to 146 °C by heat transferring with the bottom discharge of the sour water stripper and the ammonia-containing gas extracted from the side line, and then fed into the sour water stripper as hot feed.
- The bottom wastewater discharge from the sour water stripper provides heat for the reboiling flow of the solvent stripper, and then cools down to 40 °C through the hot feed stream.

- (d) The ammonia-containing gas extracted from the side line is divided into two streams through the splitter, one of which is heat exchanged with the raw material hot stream, and the other is heat exchanged with the extract of the extraction column. Two streams are combined after the heat exchange is completed and enter the first flash tank.

The parameter optimization and unoptimized heat integration process comparison is shown in Table 7.

Table 7. Comparison of heat integration results with the original process.

	Equipment Cost	Cooling Water	Low Pressure Steam (0.6 MPa)	Medium Pressure Steam (1.5 MPa)	Medium Pressure Steam (2.8 MPa)	Total Energy Consumption	TAC
	$\times 10^5$ USD	$\times 10^5$ USD/year	$\times 10^5$ USD/year	$\times 10^5$ USD/year	$\times 10^5$ USD/year	$\times 10^5$ USD/year	$\times 10^5$ USD/year
Original process	21.75	0.31	0	24.68	3.85	28.84	36.09
New process	17.80	0.05	0	22.30	2.36	24.71	30.64
Comparison	−18.2%	−83.9%	0	−9.6%	−38.7%	−14.3%	−15.1%

On the premise of considering the optimization of process parameters, the heat integration of the phenols and ammonia recovery process of coal gasification wastewater can further obtain greater room for improvement on the basis of conventional heat integration. The new heat integration process not only saves 18.2% of equipment costs, but also greatly improves the heat transfer matching between streams, which reduces the total utility consumption by 14.3%. In general, the new heat integration solution can further save 15.1% of the total annual cost compared with the conventional heat integration solution. The heat integration scheme has provided guidance for the optimization of the phenols and ammonia recovery process.

5. Conclusions

In conclusion, the present work explored the heat integration of the phenols and ammonia recovery process from coal gasification wastewater considering the changes in process parameters. The simulation and optimization of this process were carried out using Aspen Plus. A programming method for heat exchanger network synthesis based on hybrid genetic algorithm was established by Matlab, which can optimize process parameters and heat integration simultaneously.

Based on the stream information obtained from Aspen Plus simulation, the heat integration process of phenols and ammonia recovery process is designed and optimized by combining it with the heat exchanger network optimization. Taking the total annual cost after heat integration as the objective function, the following process parameters are optimized: the hot feed temperature and cold/hot feed ratio of the sour water stripper, the set temperature of the three-step partial condensation system, the feed temperature and column pressure of the solvent distillation column and the solvent stripper. The results show that the total annual cost after heat integration is the lowest when the cold-to-hot feed ratio is set to 0.15, the hot feed temperature of sour water stripper is set to 146 °C, the temperature of the three-step partial condensation system is set to 138/106/40 °C, the feed temperatures of the solvent stripper and solvent distillation column are 85/120 °C, and the column pressures are 0.8/1.2 atm. Compared with the conventional heat integration process, the total energy consumption is reduced by 14.3%, and the equipment cost is reduced by 18.2% in the new heat integration process. In a comprehensive analysis, its total annual cost was reduced by 15.1% compared with the original heat integration process.

Two principles of simultaneously optimizing heat integration and process parameters for chemical processes with column equipment are summarized by the proposed heat integration optimization method. According to these two principles, it is expected to further optimize the large-scale chemical processes with preliminary heat integration,

thereby providing theoretical guidance for the economic and environmental development of large-scale chemical processes.

Author Contributions: Q.Y.: funding acquisition, project administration, resources; J.Z.: investigation, visualization, writing—original draft; Y.L.: methodology, software; P.Y.: supervision, validation, writing—review and editing; F.W.: data curation, formal analysis. All authors have read and agreed to the published version of the manuscript.

Funding: This research was funded by the National Natural Science Foundation of China (Grant No. 22178113). And The APC was funded by Qiliang Ye.

Institutional Review Board Statement: Not applicable.

Informed Consent Statement: Not applicable.

Conflicts of Interest: The authors declare no conflict of interest.

Nomenclature

Abbreviations

MIBK	Methyl isobutyl ketone
HEN	Heat exchanger network
GA	Genetic algorithm
PSO	Particle swarm optimization
TAC	Total annual costs

Parameters and variables

H1~Hn	Hot stream
C1~Cn	Cold stream
N	Stage of heat exchanger network
T	Given temperature
i	Index of cold stream
j	Index of hot stream
k	Index of stage
C	Equipment cost
A	Cost calculation parameters
S	Heat exchanger area
n	Number of items
H	Utilities consumption
D	Column design inner diameter
N_T	Theoretical plates
T	Stream temperature
Q	Heat exchange
W	Heat capacity flow rate
y	Split flow rate
ΔT_{\min}	Minimum temperature driving force of heat exchanger
U	Heat transfer coefficient
ΔT_m	Logarithmic mean temperature difference
X_F	Independent variable of split flow rate
X_Q	Independent variable of heat load

Subscripts

H	Hot stream
c	Cold stream
hex	Heat exchanger
col	Column
s	Code of heat exchanger
u1~u4	Codes of different utilities
cu	Utility heat exchanger in cold stream
hu	Utility heat exchanger in hot stream

Superscripts

I	Initial temperature
T	Target temperature
'	Inlet temperature
"	Outlet temperature
*	Parameter flag after normalization

References

1. Yu, Z.; Chen, Y.; Feng, D.; Qian, Y. Process Development, Simulation, and Industrial Implementation of a New Coal-Gasification Wastewater Treatment Installation for Phenol and Ammonia Removal. *Ind. Eng. Chem. Res.* **2010**, *49*, 2874–2881. [\[CrossRef\]](#)
2. Busca, G.; Berardinelli, S.; Resini, C.; Arrighi, L. Technologies for the removal of phenol from fluid streams: A short review of recent developments. *J. Hazard. Mater.* **2008**, *160*, 265–288. [\[CrossRef\]](#)
3. Zhu, H.; Han, Y.; Xu, C.; Han, H.; Ma, W. Overview of the state of the art of processes and technical bottlenecks for coal gasification wastewater treatment. *Sci. Total Environ.* **2018**, 637–638, 1108–1126. [\[CrossRef\]](#) [\[PubMed\]](#)
4. Cui, Z.; Tian, W.; Fan, C.; Guo, Q. Novel design and dynamic control of coal pyrolysis wastewater treatment process. *Sep. Purif. Technol.* **2020**, *241*, 116725. [\[CrossRef\]](#)
5. Bokun, C.; Siyu, Y.; Yangyang, W.; Miyangzi, S.; Yu, Q. Intensified phenols extraction and oil removal for industrial semi-coking wastewater: A novel economic pretreatment process design. *J. Clean. Prod.* **2020**, *242*, 118453. [\[CrossRef\]](#)
6. Ruesgas-Ramón, M.; Figueroa-Espinoza, M.C.; Durand, E. Application of Deep Eutectic Solvents (DES) for Phenolic Compounds Extraction: Overview, Challenges, and Opportunities. *J. Agric. Food Chem.* **2017**, *65*, 3591–3601. [\[CrossRef\]](#)
7. Cui, P.; Chen, B.; Yang, S.; Qian, Y. Optimal design of an efficient polyphenols extraction process for high concentrated phenols wastewater. *J. Clean. Prod.* **2017**, *165*, 1395–1406. [\[CrossRef\]](#)
8. Du, S.; Wang, J.; Jin, W.; Wu, W. Complex Mechanism of Phenol Extraction of Coal Gasification Wastewater. *Pol. J. Environ. Stud.* **2019**, *28*, 1105–1113. [\[CrossRef\]](#)
9. Cui, P.; Mai, Z.; Yang, S.; Qian, Y. Integrated treatment processes for coal-gasification wastewater with high concentration of phenol and ammonia. *J. Clean. Prod.* **2017**, *142*, 2218–2226. [\[CrossRef\]](#)
10. Gai, H.; Feng, Y.; Lin, K.; Guo, K.; Xiao, M.; Song, H.; Chen, X.; Zhou, H. Heat integration of phenols and ammonia recovery process for the treatment of coal gasification wastewater. *Chem. Eng. J.* **2017**, *327*, 1093–1101. [\[CrossRef\]](#)
11. Bokun, C.; Yu, Q.; Siyu, Y. Integration of thermo-vapor compressors with phenol and ammonia recovery process for coal gasification wastewater treatment system. *Energy* **2018**, *166*, 108–117. [\[CrossRef\]](#)
12. Zahid, U. Techno-economic evaluation and design development of sour water stripping system in the refineries. *J. Clean. Prod.* **2019**, *236*, 117633. [\[CrossRef\]](#)
13. Gai, H.; Chen, S.; Lin, K.; Zhang, X.; Wang, C.; Xiao, M.; Huang, T.; Song, H. Conceptual design of energy-saving stripping process for industrial sour water. *Chin. J. Chem. Eng.* **2020**, *28*, 1277–1284. [\[CrossRef\]](#)
14. Jin, L.; Zhang, X.; Cui, C.; Xi, Z.; Sun, J. Simultaneous process parameters and heat integration optimization for industrial organosilicon production. *Sep. Purif. Technol.* **2021**, *265*, 118520. [\[CrossRef\]](#)
15. Zhuang, Y.; Zhou, C.; Zhang, L.; Liu, L.; Du, J.; Shen, S. A simultaneous optimization model for a heat-integrated syngas-to-methanol process with Kalina Cycle for waste heat recovery. *Energy* **2021**, *227*, 120536. [\[CrossRef\]](#)
16. Babaie, O.; Esfahany, M.N. Optimum process configuration for ETBE production based on TAC minimization. *Sep. Purif. Technol.* **2020**, *256*, 117744. [\[CrossRef\]](#)
17. Babaie, O.; Esfahany, M.N. Optimization and heat integration of hybrid R-HiDiC and pervaporation by combining GA and PSO algorithm in TAME synthesis. *Sep. Purif. Technol.* **2019**, *236*, 116288. [\[CrossRef\]](#)
18. Schack, D.; Liesche, G.; Sundmacher, K. The FluxMax approach: Simultaneous flux optimization and heat integration by discretization of thermodynamic state space illustrated on methanol synthesis process. *Chem. Eng. Sci.* **2019**, *215*, 115382. [\[CrossRef\]](#)
19. Huang, B.; Li, Y.; Gao, R.; Zuo, Y.; Dai, Z.; Wang, F. Simultaneous optimization and heat integration of the coal-to-SNG process with a branched heat recovery steam cycle. *Comput. Chem. Eng.* **2018**, *117*, 117–128. [\[CrossRef\]](#)
20. Khor, C.S.; Elkamel, A. Optimal synthesis of a heat-integrated petroleum refinery configuration. *Can. J. Chem. Eng.* **2016**, *94*, 1939–1946. [\[CrossRef\]](#)
21. Soares, A.D.F.; Penteadó, E.D.; Diniz, A.A.R.; Komesu, A. Influence of operational parameters in sour water stripping process in effluents treatment. *J. Water Process Eng.* **2021**, *41*, 102012. [\[CrossRef\]](#)
22. Gai, H.; Song, H.; Xiao, M.; Feng, Y.; Wu, Y.; Zhou, H.; Chen, B. Conceptual design of a modified phenol and ammonia recovery process for the treatment of coal gasification wastewater. *Chem. Eng. J.* **2016**, *304*, 621–628. [\[CrossRef\]](#)
23. Khalili, N.; Kasiri, N.; Ivakpour, J.; Khalili-Garakani, A.; Khanof, M. Optimal configuration of ternary distillation columns using heat integration with external heat exchangers. *Energy* **2019**, *191*, 116479. [\[CrossRef\]](#)
24. Beninca, M.; Trierweiler, J.O.; Secchi, A. Heat integration of an Olefins Plant: Pinch Analysis and mathematical optimization working together. *Braz. J. Chem. Eng.* **2011**, *28*, 101–116. [\[CrossRef\]](#)
25. Lewin, D.R. A generalized method for HEN synthesis using stochastic optimization—II.: The synthesis of cost-optimal networks. *Comput. Chem. Eng.* **1998**, *22*, 1387–1405. [\[CrossRef\]](#)

26. Ulyev, L.; Kanishev, M.; Chibisov, R.; Vasilyev, M. Heat Integration of an Industrial Unit for the Ethylbenzene Production. *Energies* **2021**, *14*, 3839. [[CrossRef](#)]
27. Yee, T.F.; Grossmann, I.E.; Kravanja, Z. Simultaneous optimization models for heat integration—I. Area and energy targeting and modeling of multi-stream exchangers. *Comput. Chem. Eng.* **1990**, *14*, 1151–1164. [[CrossRef](#)]
28. Rathjens, M.; Fieg, G. A novel hybrid strategy for cost-optimal heat exchanger network synthesis suited for large-scale problems. *Appl. Therm. Eng.* **2019**, *167*, 114771. [[CrossRef](#)]